Correlations the Interplanetary Characteristics and the Occurrence of Geomagnetic Large Storms

Pawan Kumar[1], Mahender Pal[1] and Sham Singh*[2]

[1]Department of Physics, IKG Punjab Technical University, Jalandhar-144603

[2]Department of Applied Sciences, Chandigarh Engineering College-CGC Landran, Mohali, Punjab-140307

DOI: 10.54882/14202414202317855

Abstract

The research work intends to investigate the correlations and interaction between interplanetary characteristics and the occurrence of geomagnetic large significant storms. Using the Dst index hourly data, Kp and solar wind measurements from various satellites and review the chain of events that happened on March 17, 2015, December 20, 2015,September 8, 2017and August 26,2018 with Dst values of -234 nT,-155 nT,-124 nT and -175 nT, respectively. Strong magnetic storms are mostly caused by high-speed solar ejectors and too-fast coronal mass ejections, whereas there is a strong positive association between solar wind speed and solar wind proton density and AE indices. Furthermore, there is a strong positive correlation between SSN and F10.7 values, polar cap values, and proton densities. The results will advance our knowledge of space weather dynamics by offering insightful information on the connections between solar wind and disturbance features. The results will advance our knowledge of space weather dynamics by offering insightful information on the connections between solar wind and disturbance features.

Keywords: Coronal mass ejection, geomagnetic storm, interplanetary parameter, and space weather.

1.0 Introduction

The magnetosphere of Earth is disturbed by the irregular Alfvenic wave and supersonic flow of magnetised plasma that the sun released in the outer atmosphere and spread throughout interplanetary space. The relationship between the sun, , and earth space related phenomena that may exist, such as space weather,

The solar wind velocity and the interplanetary magnetic field(Bavg) both increase the intensity of a geomagnetic storm on Earth[24]. Many authors have provided explanations of the various geomagnetic storm types and their causes. geomagnetic storms are usually associated with a sunspot number (SSN), magnetic cloud rather than a solar flare. To further explore the effectiveness of solar and interplanetary parameters, we have analysed the effects of major events by examining various interplanetary parameters. The events have been classified according to the magnitude of the strength of geomagnetic storms[1].

Magnetic storms are a major factor in disturbing the shape of the magnetic sphere of the earth. We can observe the extent of ring current measured with the DST [5,6,10,12].A CME's eruption can contain a billion tonnes of matter that can speed up its velocity up to several million miles per hour. CME originates from the solar disc and harms the earth's environment and causes mass ejection from the sun in a range of 10^{10} kg[15].

The solar wind effect the magnetospheric and ionosphere current systems [19] and ring current intensity and storm severity are both determined using the DST index[5].

Through magnetic reconnection on the dayside of the magnetopause, a significant amount of magnetic and kinetic energy from the solar wind was transported to the Earth's magnetosphere. It happens when the geomagnetic field and IMF are in opposition to each other in the south. In order to explore the relationship between the sun's activity driver and the magnetospheric response for space weather prediction, magnetic energy rather than sun wind pressure works as a significant factor [27].The previous study demonstrates that

CME, ICME, and the solar wind's interaction with the earth's magnetosphere during geomagnetic storms, and superstorms, as well as high-intensity, long-duration continuous auroral activity (HILDCAA), are the main drivers of geomagnetic storms [16].
Singh ,2020study discovered a delay in total electron content (TEC) response during the flares peak time as well as recovery time, as well as an increase in total electron content during day time hours and a small decrease or no change during night hours during a solar flare[25]. Other factors that cause vertical magnetic field drift of the ionosphere include the solar zenith angle and active region location at the sun's surface, a time delay is observed in total electron content response to its maximum value. Plasma solar flare provide additional ionisation, and their effect is more pronounced in the atmospheric layer. Pokharia(2021) observed that high-speed solar wind streams have a higher correlation coefficient than slow solar wind streams [22]. According to Pokhariya, there is a one-day time lag between the peak value of high-speed solar wind and the IMF. Tariq [28] investigated the geomagnetic field and high-speed solar wind stream during the period of solar storm induced by the coronal stream. During the study period, DST is used to check the level of geomagnetic strong and ring current activity because the interaction take place between the high-speed solar wind magnetic field and Earth magnetic field .

Numerous studies have found links between the frequency and intensity of geomagnetic storms and particular characteristics of the solar wind, such as its speed, density, and orientation with respect to IMF value [10,11,17]. The solar wind, a never-ending stream of charged particles emanating from the Sun, interacts with the Earth's magnetosphere to produce these storms. For improving space weather forecasting and reducing the negative consequences of these occurrences, research into the connections between big geomagnetic storms and interplanetary parameters is essential.
Solar flares and coronal mass ejections (CMEs) are two solar activities that release a significant amount of energy and magnetised plasma into the interplanetary medium [2]. According to Gopalswamy, 2006[14]these disturbances interact with the Earth's magnetosphere as they move towards the planet, causing dynamic changes in its magnetic field and the induce strong electric currents. These interactions cause geomagnetic storms to form, which can last for several hours or days./). Interplanetary parameter of space weather and some geomagnetic indices taken as Dst, AE index, and polar cap are studied [3,4].
The solar and interplanetary parameters that disturb the magnetosphere explained in this work provide a better expectation for understanding space weather than old work [20,23,30].
The objective of the statistical study presented in the paper is to explain how interplanetary space weather a cause major geomagnetic storms that are hazardous to our communication system .The research work seeks to identify statistically significant correlations and interaction between interplanetary parameters (such as SSN, CME properties, solar wind, and IMF components) and the occurrence geomagnetic large major storms.

2.0 Data Selection and Methodology

Geomagnetic storms with decrease of |Dst| value have various class as -100nT<Dst<-50nT, -200nT<DST<-100nT, -300n<Dst<-200nT, Dst<-300nT, which are classified according to Gonzalez[12,13].Rating the geomagnetic storm as moderate, strong, severe and great based on the value of the Dst value during geomagnetic storm occurrences, in accordance with Cander and Mihajlovic's study[9].Solar and geomagnetic index data are available at http://OmniWeb.gsfc.nasa.gov/ King & Papitashvili(2005)[18]. The Soho satellite's Lasco telescope regularly observes CMEs[7]. CME analysis is aided by the website www.cdaw.gsfc.gov.in.CMEs create geomagnetic storms and usually reach Earth within 2–5 days[14].The interplanetary medium's CME sheath and ejecta are dominating where this occurs [8]. Shock waves travel an astronomical distance in 33 hours due to the CME that propels them. A slow CME can travel to the surface of the Earth for up to 6 days, counting the day of emission. The world data centre (WDC) in Kyoto can be used to record DST data (swdcwww.kugikyoto u. ac.jp

3.0 Result and Discussion

This work attempt to investigate the significant of geomagnetic storm as it relates to solar indices and interplanetary disturbance characteristics. The largest interplanetary disruption is caused by CMEs and fast solar wind, which accelerate the magnetosphere's Aurora and ring current as well as energies the Solar energetic particle and increases particle precipitation in the Earth's atmosphere.

Overall, the research reveals that the bulk of storms that were observed into the moderate category, with fewer storms falling into the strong category and very few storms falling into the severe category. However, no large or extremely strong storms were seen throughout the time period that was reported.

The frequency of sever geomagnetic storms is greater at their peak, while there is a low frequency of storms during the minimum of the cycle. During the descending part of the solar cycle, the slow and rapid solar radiation, CMEs, and other associated structures are the primary drivers of geomagnetic storms., which are strongly dominated by strong and moderate storms. Additionally, we discovered that strong and intense storms frequently develop close to the Solar Maxima peak.

Table1 Characteristics Feature of Major Solar and Geomagnetic Parameters Selected for Analysis of Geomagnetic Storms During the Year 2015-2018.

Date & value of min. Dst	Date of CME	CME speed & its type km/s	Solar Wind Velocity (Km/s)	IMF Bavg, nT	Plasma density (n/cc)	Kp	SSN	F10.7 (Sfu)	AE (nT)	Polar Cap
Mar 17, 2015 (-234 nT)	2015/03/15	719 H	544	20.9	6.4	77	38	113.2	1168	9.8
Dec 20, 2015 (-155 nT)	2015/12/19	797 PH	415	18.7	6.6	63	21	112.8	695	5.9
June 01, 2016 (-116 nT)	2015/05/29	1212 H	463	15	2.0	60	37	95	686	4.4
May 28, 2017 (-125 nT)	2017/05/27	845 PH	369	16.9	8.4	60	21	81	1083	5.7
Sep 08, 2017 (-124nT)	2017/10/06	441 PH	724	7.3	3.1	73	88	118.5	851	5.0
Aug 26, 2018 (-175 nT)	2017/08/24	229 PH	378	17.7	2.3	73	28	72.6	987	5.8

The given table provides information about various solar and geomagnetic parameters selected for the analysis of stronggeo storms having |Dst| < -100 nT during the period from 2015 to 2018.

Numerous geomagnetic storms with minimum Dst values less than -100nT have been seen, according to the examination of the data presented. CME characteristics, solar wind velocity, IMF Bavg values, plasma densities, Kp indices, SSN values, F10.7 values, AE indices, and polar cap values shown all related with these storms. The findings provide insight into the frequency and features of geomagnetic storms within the time periods specified. When several successive strong CME hits the magnetosphere of the earth, the Dst < -200 nT, and extreme storms may be triggered, also known as outstanding sun-earth connection (OSEC). These events usually happen around the peak of the Sun cycle, so to more study of the effect and production of geomagnetic storms before 2 years or after three years.

3.1 Solar Activity 17thMarch 2015

A severe geomagnetic storm with a minimum Dst value of -234nT occurred on March 17, 2015. On March 15, 2015, a CMEs with a velocity of 719 km/s was recorded, and a H(Halo) CME was linked to this storm. During this time, the average IMF Bavg was 20.9 nT, and the high solar wind's speed recorded ~ 544 km/s. The density of the plasma was 6.4 n/cc. The Kp index, which peaked at 6.4 during this storm, was used to gauge the geomagnetic activity. The F10.7 (Solar Radio Flux) was 113.2 and the SSN (Sunspot Number) was 77. The polar cap was 9.8 and the AE index, which measures auroral activity, was 1168.

The principle causes of intense magnetic storms are rapid CMEs and high-velocity solar ejecta, which are responsible for the forward shock wave. Geomagnetic storms were seen on March 17, 2015, with Dst< -234 nT peaking at 23.00 UT. The two major factors that transform a storm into a moderate and intense one is high-speed solar wind and CIR. In addition, ICME is crucial for the development of powerful storms. As of March 15, 2015, an extremely swift HALO CME was seen, and it happened at 1.48 UT. The CME's peak was at 2.13 UT, and it was caused by a C9.1 solar flare that originated from active area 12297 at the sun's surface (S22W25). On March 14, 2015, a C2.6-type solar flare that originated from the active zone and peaked at 11.55 UT was also related to a HALO CME.

The effect of interplanetary disturbance variation produces hydrodynamic plasma waves that propagate through the magnetosphere of the earth The study of SEP > 10 MeV and their associations with solar flares and other activity are crucial to understanding perturbance in space weather [26]. Examined the flare size, source location, and CME characteristics of the associated SEPs that can be generated by a shock wave driven by a CME when the CME speed exceeds the coronal sound speed. They make a SEP type II radio burst because of the shock wave that forms ahead of the CME during the eruption, and they make a SEP type III because of magnetic reconnection. In the top part of this data visualisation, solar energetic particles (SEPs) found by the GOES satellite are shown in three energy bands (10, 50, and 100 MeV). In the middle picture, you can see the height-time profile of a coronal mass ejection (CME) that was measured by LASCO. The colours in the middle panel show the main way in which a CME moves. The bottom panel shows the total soft X-ray (SXR) emission from the flare, which was measured by GOES between 0.5 Å -4.0 Å and 1.0 Å -8.0 Å.

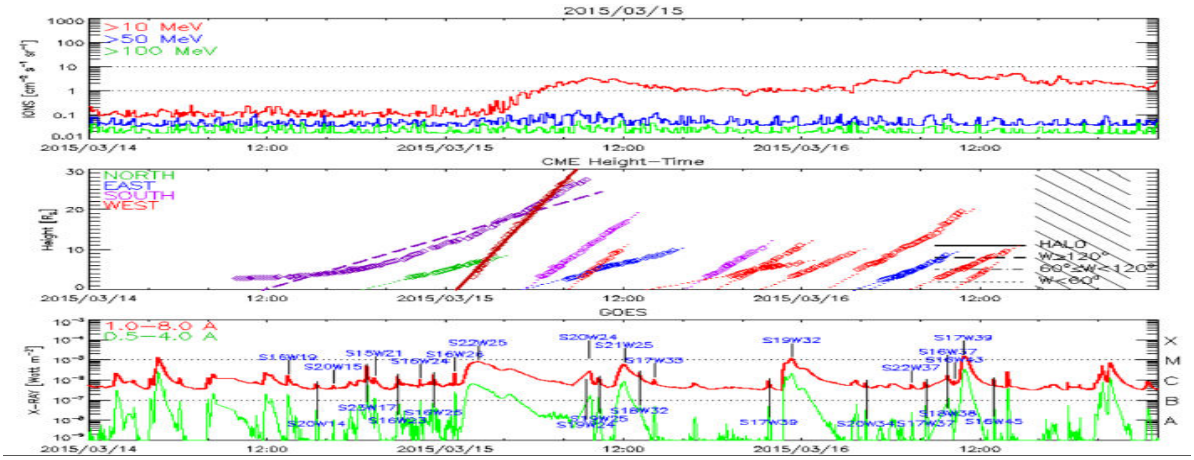

Figure 01 shows the PHTX plot for the time period of March 15, 2015;

Figure 01 uses data from the proton-height/time-X-ray (PHTX) plots in the CDAW (Coordinated Data Analysis Workshop) library, which can be found at https://cdaw.gsfc.nasa.gov/CME r [29,19]. Also, the Dst (Disturbance storm time) index shows that the interplanetary coronal mass ejection (ICME) caused the strong magnetic storm on March 17, 2015.The core area of the shock wave also makes a difference in the second and third times the Dst index goes down because of an ICME. On March 15, 2015, a solar flare of type X2 that was connected to a HALO CME was seen. The average value B also grew from 7.62 nT to 31.8 nT, and the DST index value reached a value of -234 nT.

High-speed solar ejectors and too-fast CMEs are the main contributors to strong magnetic storms. Energy is what causes both the high interplanetary magnetic field pointing southward and the increased plasma pressure brought on by the solar wind's acceleration behind the shock wave. Magnetic reconnection take place between the IMF (Bavg) and the Earth's magnetic field, which is cause of transferring energy from the external solar environment to the earth's magnetosphere. ICME type magnetic cloud and ejecta are the sources of geomagnetic storms[4].

The recovery phase begins when IMF moves less southward after a delay of one hour. The recovery phase, which physically results from the combination of multiple separate energetic particle interaction processes such as Coulomb collision, charge exchange, and wave-particle interaction during the solar minimum, has a decay period of 10 hours. The interplanetary medium's activity is mostly dominated by a fast stream from the corona hole. High solar wind density and low-speed stream recombination with the HALO, a spherical plasma sheet impinging on the magnetosphere of earth, are the primary causes of the early phase. During this stage, sudden impulses are rare. The HCS plasma sheet interacts with a rapid coronal hole stream to produce strong field regions known as CIR regions. The magnetic storm's primary features have extremely regular magnitudes that are also excessively flexible in the Bz component. The phase of recovery can persist for several days to a week. Reconnection happens as a result of the magnetic field component of an alpha wave during a fast stream. Its final decay values are prolonged by a series of substorms and a regular infusion of plasma sheet energy into the outer part of the ring current. High-intensity, long-duration continuous Arora electrical activity(HILDCA) is the term used to describe the ongoing Arora activity.If the speed difference between the corona ejecta and the slow upstream solar wind is larger than the magneto sonic speed[12] the first CME, which has a speed >500 km/s and a strong magnetic field, can be seen at one astronomical unit.

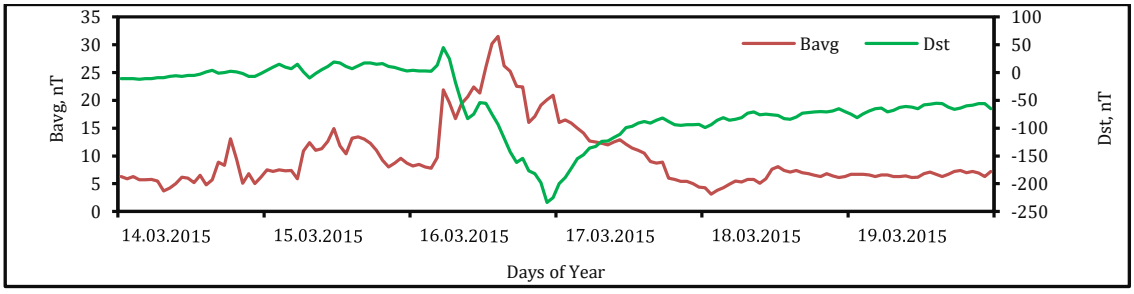

Fig.2 (a)

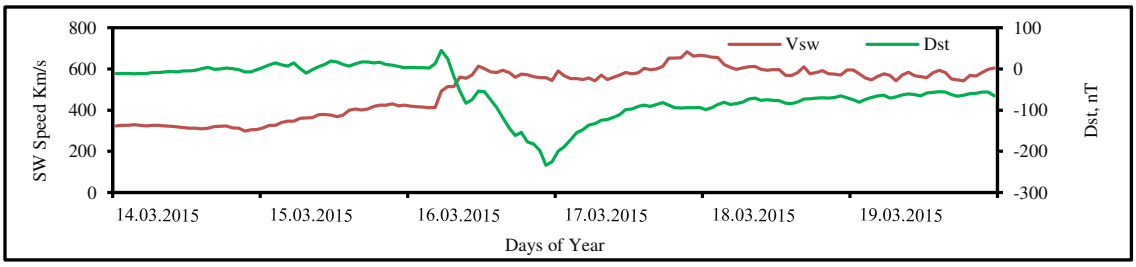

Fig.2 (b)

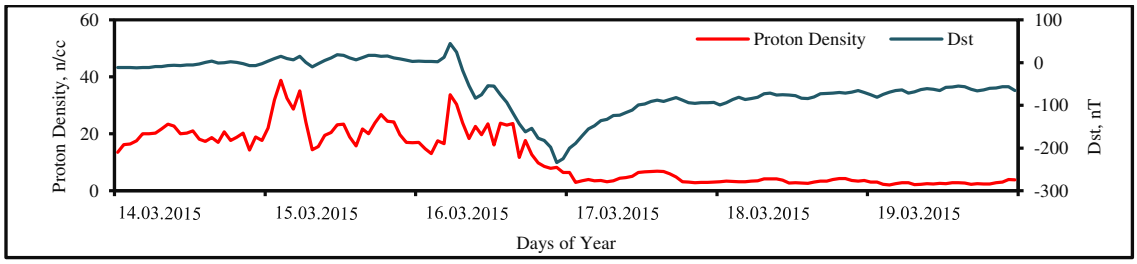

Fig.2 (c)

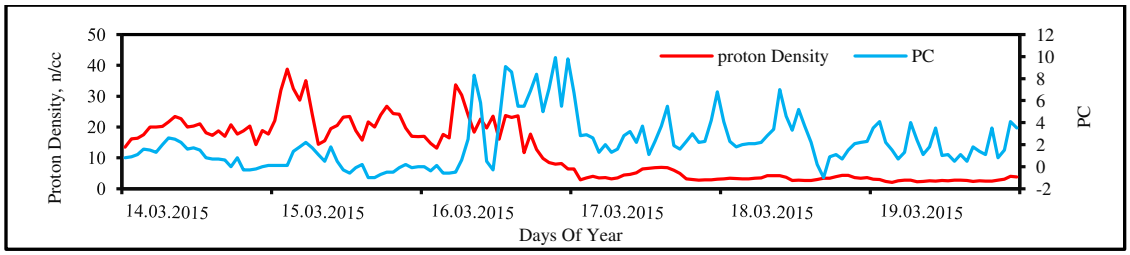

Fig.2 (d)

Figure2. Geomagnetic indices and interplanetary parameters related to the severe geo storm |Dst|<-234 nT on March 17, 2015, showing (a) IMF with the storm index Dst index, (b) solar wind speed (red) with the Dst curve (green) , (c) solar wind density with Kp, and (d) solar wind density with PC during March 14–19, 2015.

From March 14 through March 19, 2015, Fig. 2(a) shows the interplanetary magnetic field(Bavg) in relation to the negative of Dst value. According to statistics, there are fewer geomagnetic storms that are more powerful (Dst magnitudes of -234 nT). Bavg value reached 31 nT before some hours and 20.9 nT during storm time and became normal after two days. Fig. 2(b) shows the variation between solar wind speed and Dst during the period of March 14 to March 19 in the year 2015. The velocity of the solar wind increases to 595 km/s near 10 hours after onset. The value reaches 544 km/s during the storm, and the fluctuation continues for the next 2 days. Fig. 02(c) Shows the variation between solar wind density and Dst during the time period of March 14

to March 19 in the year 2015. The solar wind density becomes more turbulent and irregular about 1 day before the geomagnetic storms while During storm time, Dst events decrease very rapidly and reach -234 nT.Fig. 02(d) shows the plot between the polar cap and solar wind proton density during March 2015. The proton density increased irregularly and turbulently 24 hours before the storm. The polar cap also irregularly increased for about 8 hours before the storm and became normal after the storm event passed.

Fig. 03(a) shows the variance and correlation between Dst and Bavg for March 14–19, 2015. In this graph, there is a linear connection between Bavg and Dst, indicating that the strength of geomagnetic storms is averagely dependent on the value of the Bavg. The correlation coefficient was measured - 0.65, which is a moderate correlation value.Fig. 3(b) shows the variance and correlation between DST and solar wind speed for 14-19 March ,2015. R^2 represents the variance of 52.31% between both parameters, and the negative correlation coefficient is -0.72.Fig. 03(c) shows the correlation between solar wind proton density and Dst 14-19 March 2015, and it is discovered that there is a strong association between the two variables. The correlation coefficient between the values is 0.65, and the R^2 value reflects the variance between the two parameters, which is 41.79 percent.

The link between the polar cap and solar wind proton density between March 14 to March 19, 2015, is depicted in Fig. 3(d). The correlation coefficient between proton Density Vs PC values is - 0.24.

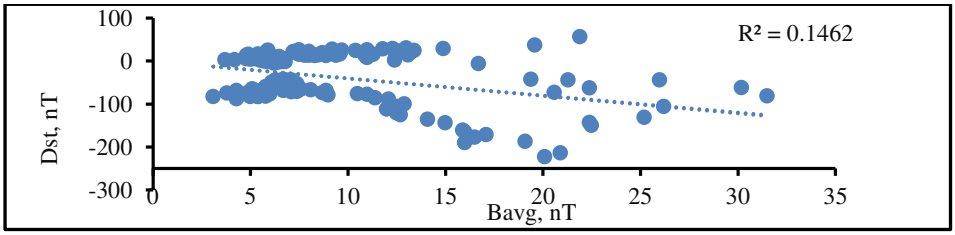

Fig. 03(a)

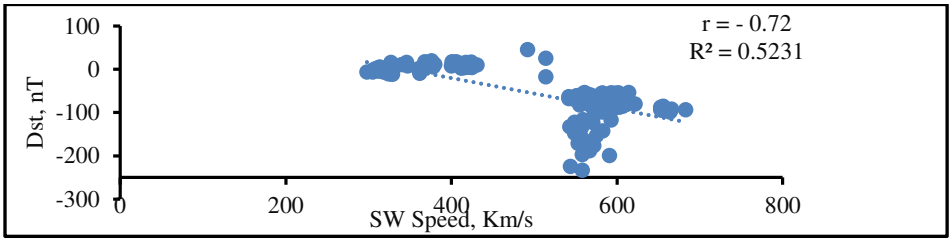

Fig. 03(b)

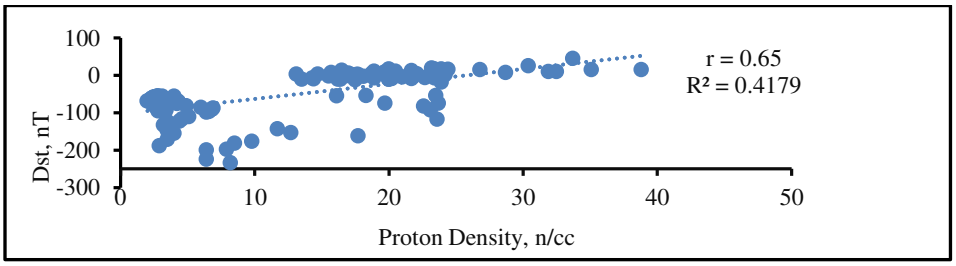

Fig. 03(c)

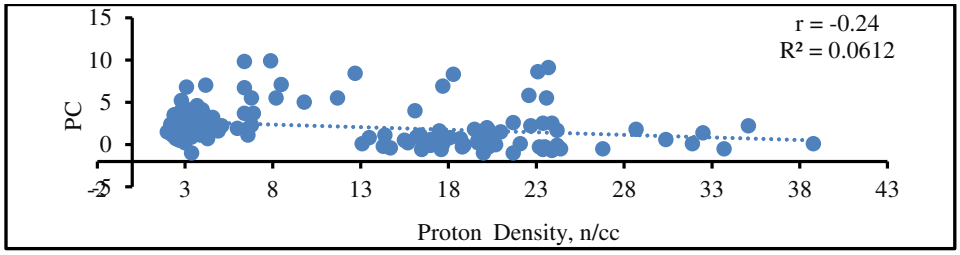

Fig. 03(d)

Fig. 3. Correlation coefficient plot of daily observed values of interplanetary parameters and geomagnetic indices for (a) Bavg vs. Dst; (b) Solar wind speed vs. Dst;(c) Solar wind proton density vs. Dst during March 14–19.Fig. 04(d)Correlation plots Solar proton density with polar cap during the period March 14–19, 2015.

3.2Solar Activity 20th December 2015

A CME(PH) with a speed of 797 km/s that was recorded on December 19, 2015, was connected to this strong storm. During this time, the average IMF Bavg was 18.7nT, and the solar wind's speed was 415 km/s. The density of the plasma was 6.6 n/cc. A value of 6.6 for the Kp index indicates moderate geomagnetic activity. The F10.7 was 112.8, and the SSN was 63. The polar cap was 5.9 and the AE index was 695.

The DST index profile explains the magnetic storm in December 2015 by reaching Dst value of -155 nT. A HALO CME associated with solar flare C 6.6, which was produced from active region 12468 at latitude S14W20, was visible on December 16, 2015, around 9:36 AM. After some time, SOHO/LASCO found a HALO CME. The second row is visible in the DST time profile; DST occurs in a sheath region; soft X waves arrive at 81 AU when the interplanetary coronal mass ejection boundary is crossed; and the Bz value shifts more negatively when alternate series of CME are acting to produce a complex magnetic storm or are rejected that have a longer time span, all of which are characteristics of the best decrease value.The storm is the result of a series of powerful and swift CMEs, whose corresponding IP shocks leave distinct signatures in the in situ plasma and the groundbased geomagnetic field [2].

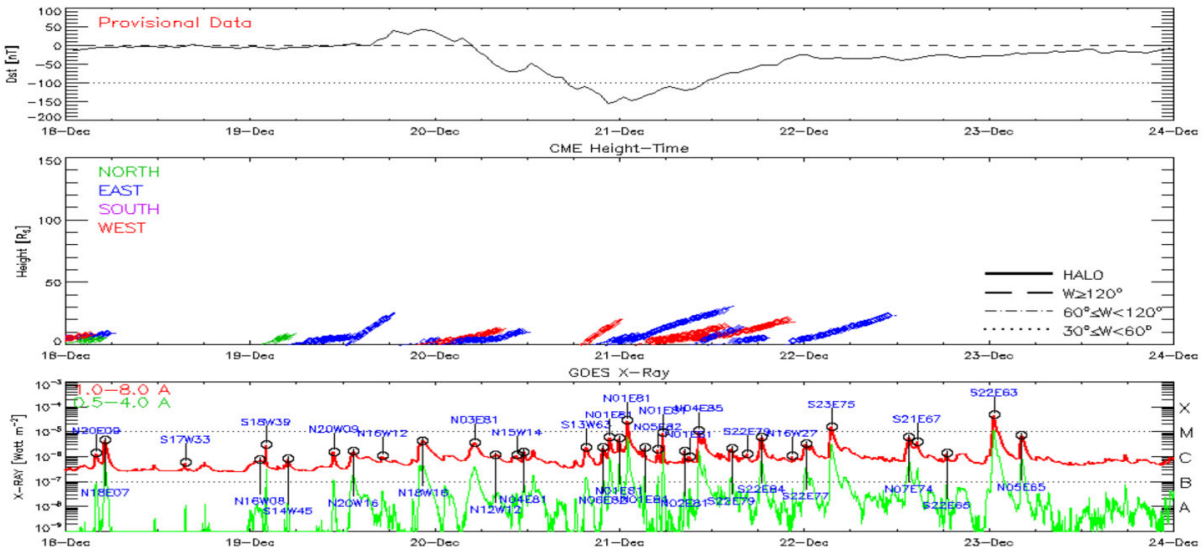

Fig. 4Dst index (top), coronal mass ejection (middle), and GOES soft X-ray light curves (bottom) plots.

Including data on proton energetic particle events, LASCO instrument observations, and GOES flare SXR emission, the above plot describes a revised version of the X-Ray -CME-SEP series from the "CDAW" catalogue for September 2017. LASCO's measurements of the CME's height over time are shown in the middle panel, with different colours denoting the principal propagation direction (for further information, see the legend on the panel's left side). Finally, the SXR emission from the combined GOES flare is shown in the bottom panel, spanning from 0.5 to 4.0 *Å* and 1.0 to 8.0*Å* in wavelength. The PHTX charts at https://cdaw.gsfc.nasa.gov/CME_list contain additional information and more in-depth visual representations. The first peak was seen as a result of CME activity, but the second peak was brought on by the fast plasma speed.

IMF (Bavg) and DST variation from December 18 to December 23, 2015, is depicted in Fig. 10(a). The interplanetary magnetic field is plotted against the maximum of negative Dst in Fig. 10(a). According to statistics, the 20th of December 2015 shows the occurrence of more powerful geomagnetic storms having Dst value reaches to -155 nT. The interplanetary field value Bavg increased dramatically the day before the storm. It swings erratically within two days throughout the storm's main phase [31]and typically follows the recovery phase of a magnetic storm . A peak at 14.9 nT with positive Dst may be seen on December 19. The Bavg value for the 23 hours of December 20 was 18.7 nT, and the Dst value is -155 nT. Peak Bavg is 19.5 nT with DST value changing to -151 nT during Dst recovery.

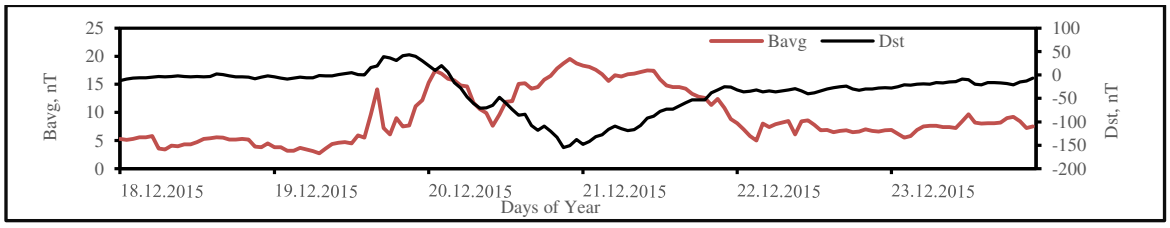

Fig. 05(a)

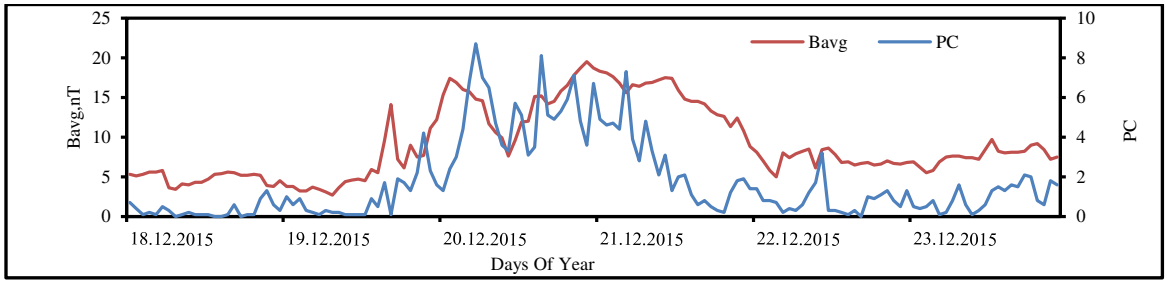

Fig. 05(b)

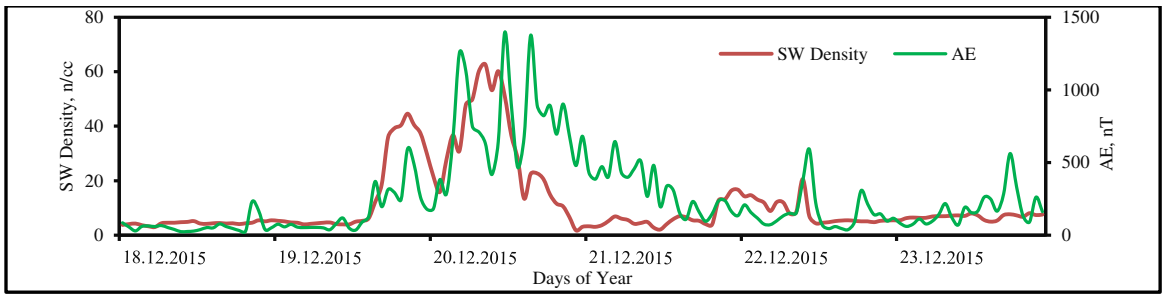

Fig. 05(c)

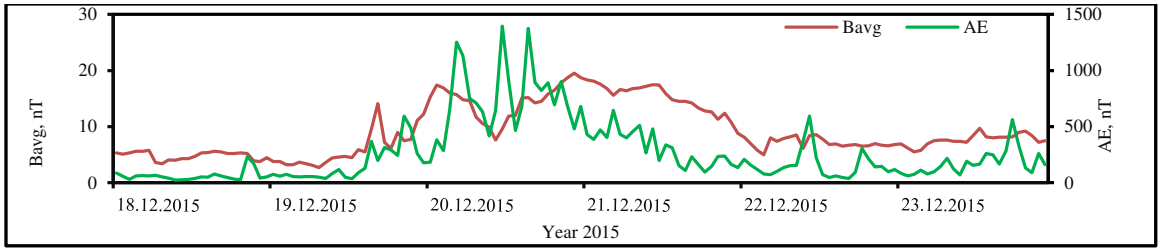

Fig. 05(d)

Figure 05. From top to bottom, thepanelsshow the Geomagnetic and interplanetary parameter connection to the strong geomagnetic storm (Dst < -155 nT) on 20 December, 2015, showing (a)IMF Bavg with the storm index Dst index, (b)IMF Bavg with PC (c) solar wind density with AE and (d) Bavg with AE during 18-23 December, 2015.

The geomagnetic storm's main phase started with the southward turning of the Dst index at 400 UT on December 20. The main phase ended at 2300 UT on December 20, when the DST value reached -166 nT, and the DST value returned to normal after the recovery phase began. On December 20, 2015, at 2200 UT, Dst reaches -170 nT at night, and the maximum increase in TEC is 35. Due to the sheath CME, there was a large amount of intense magnetic activity. This caused a geomagnetic storm, which is a temporary change in the earth's magnetic field caused by CMEs and solar flares.

IMF (Bavg) and DST variation from December 18 to December 23, 2015, is depicted in Fig. 05(a). The interplanetary magnetic field is plotted against the maximum of negative Dst in Fig. 05(a). The Interplanetary magnetic field vs the maximum polar cap from 18 to 23 December 2015 is depicted in Figure 05(b). On December 20, 2015, more severe geomagnetic storms (negative Dst magnitudes -155 nT) occurred statistically. Before 1 day of the storm, the interplanetary field value Bavg increases very rapidly. During the main phase of the storm polar cap (PC)changes irregularly and comes normally after the recovery phase of a magnetic storm. When the IMF magnetic field value became 16.9 nT, after 1-hour polar cap value reaches its peak value of 8.7 before the intense storm. Figure 05(c) shows the variation of SW proton density versus the maximum AE. Solar wind density on 20 December reaches 62.7 n/cc, Then the AE value goes to 640 nT. After 6 hours AE

value reaches 1396 nT. Next peak value reaches to1375 while solar wind density is 22.5 n/cc. It is clear that higher values of solar wind density are not always related to stronger geomagnetic storms. This indicates that there is a strong likelihood that the higher density will not affect the strength of a geomagnetic storm[20].Fig. 05(d) displays interrelation between the maximum AE with Bavg. According to statistics, the 20th of December 2015 saw the occurrence of more powerful geomagnetic storms, with| Dst| recorded to -155 nT. The average interplanetary field value (Bavg) changes drastically just one day before a storm. During the storm's main phase, AE also gets close to 1396 nT, fluctuates erratically, and typically follows the storm's recovery phase [26].

Figure 6 (a) demonstrates the relationship between the IMF Bavg and the Dst value. There is a negative correlation between the parameters. These two parameters have a correlation value of -0.72. Figure 6(b) displays the relationship between the IMF Bavg and the polar cap. There is a good positive correlation between the two of these characteristics. These two parameters have a correlation value of 0.72. The proton density is plotted against the Aurora electrojet in figure 6(c). It is discovered that there is a clear association between the two variables. There is a 0.57 correlation between the two of these factors. The relationship between IMF Bavg and aurora electrojet is depicted in Figure 6(d) (AE). There is a positive correlation between the two of these characteristics, with a value of 0.62.

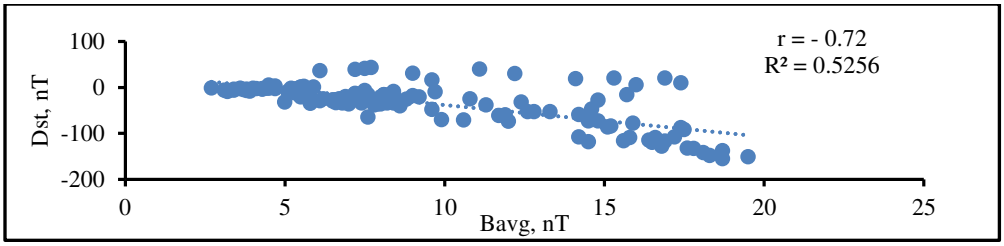

Fig. 10(a)

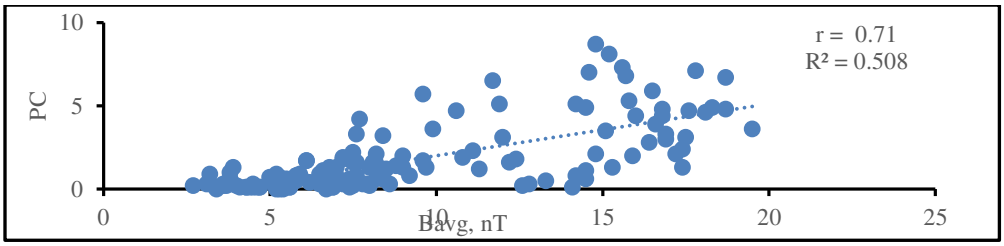

Fig. 10(b)

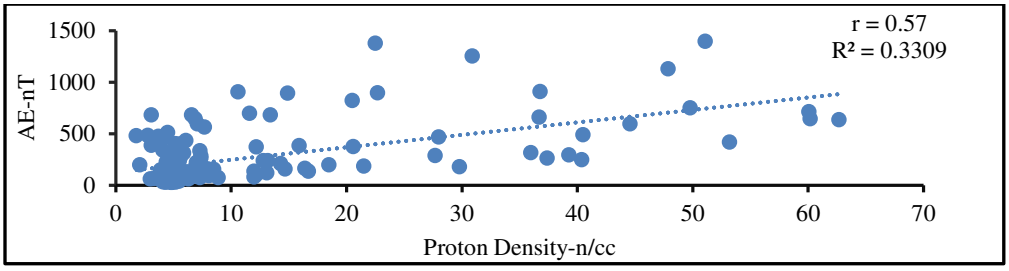

Fig. 10(c)

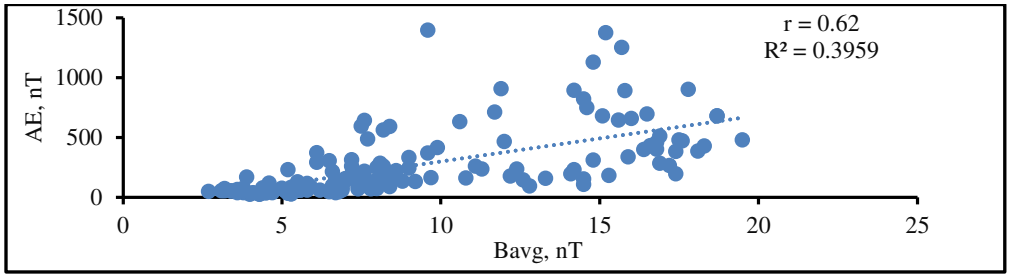

Fig. 6(d)

Fig. 6 Correlation coefficient plot of daily observed values of interplanetary parameters and geomagnetic indices for (a) Bavg Vs Dst; (b) BzVs PC; (c)Proton Density Vs AE (d)Bavg Vs AE

3.3Solar Activity in 8th September 2017

Between September 6 and September 8, 2017, a series of powerful flares were released from the sun's active area as a result of the intense magnetic flux being ejected. A very powerful geomagnetic disturbance with a minimum Dst of -124 nT. A powerful HALO CME was seen on September 6, 2017, at 12:24:05 UT, with a first appearance CMEs speed of 1571 km/s and a space speed of 1819 km/s. A strong X 9.3 flare that reached a DST of -124 nT was seen at a site that had a strong CME.

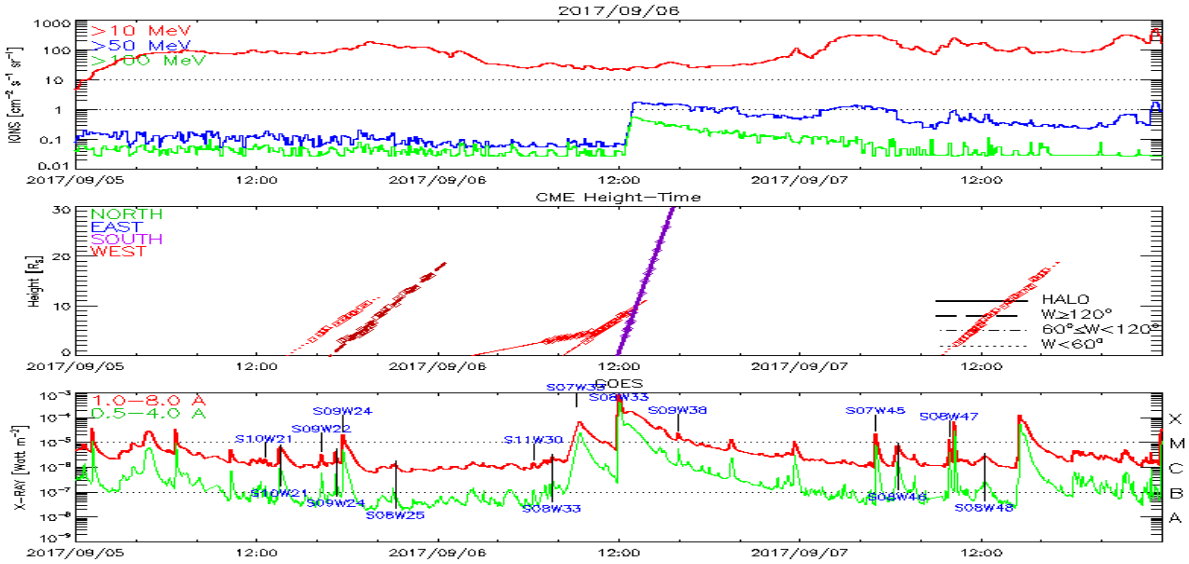

Fig. 7 Flare-CME-SEP series for September 2017 recovered from the CDAW database (proton-height/time-X-ray graphs are available at https://cdaw.gsfc.nasa.gov/CME list.

The top panel depicts proton occurrences of solar energetic particles in GOES ion energy channels 10 MeV, 50 MeV, and 100 MeV. The middle panel depicts the CME height-time profile as recorded by LASCO (colours indicate the predominant propagation direction; see legend to the left of the middle panel[29]The bottom panel displays the combined 0.5–4.0 *Å* and 1.0–8.0 *Å* GOES flare SXR emission disc.

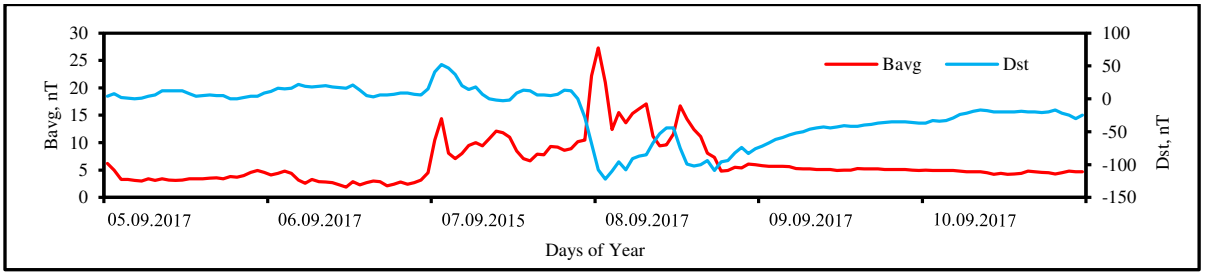

Fig.8(a)

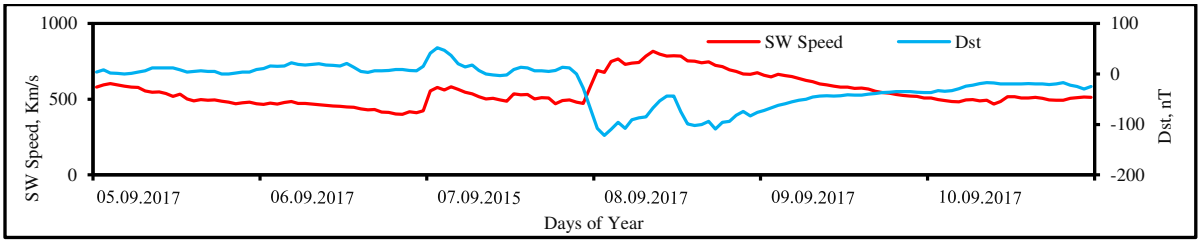

Fig.8(b)

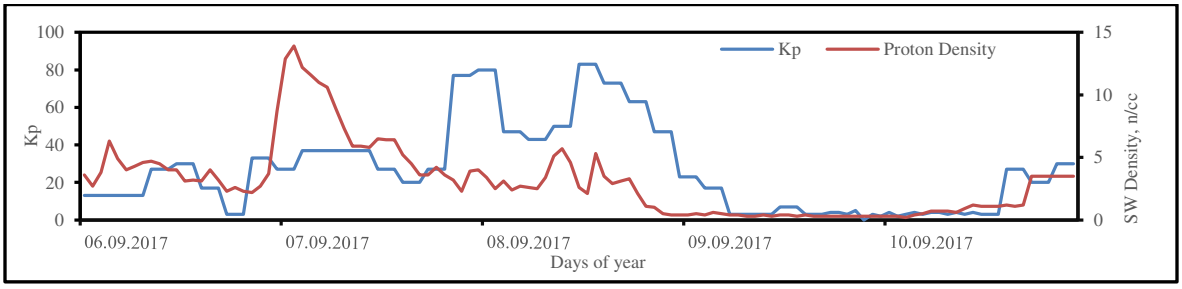

Fig.8(c)

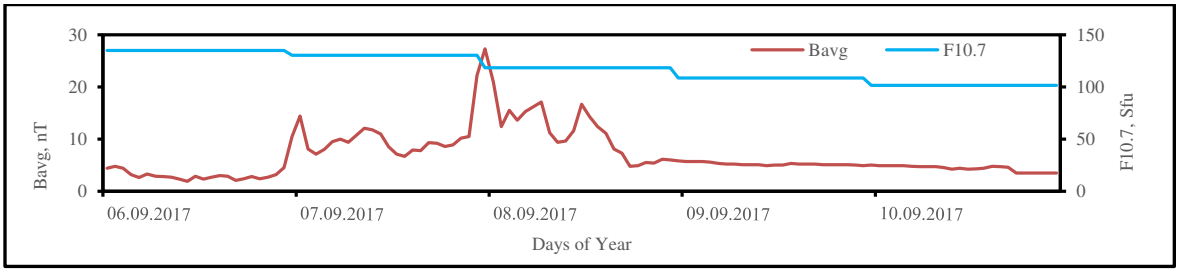

Fig. 8(d)

Figure 8: From top to bottom, the panels show the variations of the IMF Bavg Vs Dst, Vsw (Km/s) Vs Dst, Nsw (n/cc) Vs Kp during 5-10 September, 2017.

Fig. 8(a) displays the interplanetary magnetic field in relation to the highest possible negative Dst. According to statistics, the day of September 8 saw the occurrence of more powerful geomagnetic storms with Dst values below -124 nT. Bavg, the interplanetary field value, grows quite quickly before the storm. It begins to fluctuate erratically about one day into the storm's main phase before returning to normal during the storm's recovery phase [26].

Figure 8(b) depicts the SW speed in relation to the greatest Dst (negative). There is a strong link between these two characteristics. It can be shown that geomagnetic storms with greater strength are necessarily connected with higher values of Speed. This indicates that there is a high possibility that the increased velocity determines the intensity of a geomagnetic storm. 0.77 is the correlation coefficient between these two factors. The graph depicts the greatest values of solar wind velocity vs negative Dst (max.). The dispersion is more extensive, with

speeds ranging from 400 to 800 km/s. Greater geomagnetic storm intensities (peak Dst -124 nT) are not associated with higher solar wind velocity.The SW proton density is shown against the planetary index Kp in Figure 8 (c) [4].There is a strong correlation between the two of these characteristics. It is clear that higher values of solar wind density are linked to stronger geomagnetic storms. The solar wind density dramatically increased before one day, but the Kp index did so six hours before geomagnetic storms. One day later, the Kp index returned to normal. These two parameters have a correlation value of 0.69.

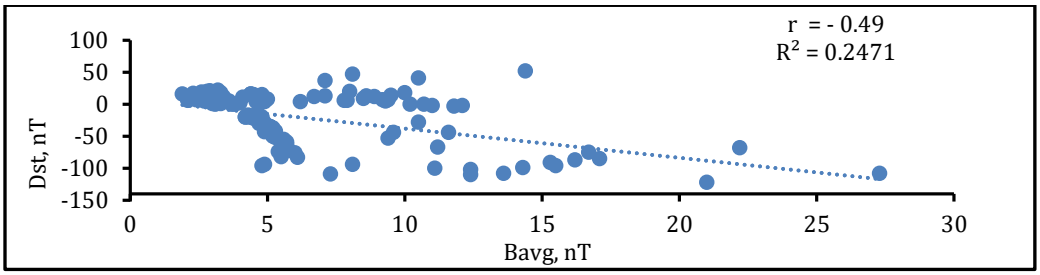

Fig. 9(a)

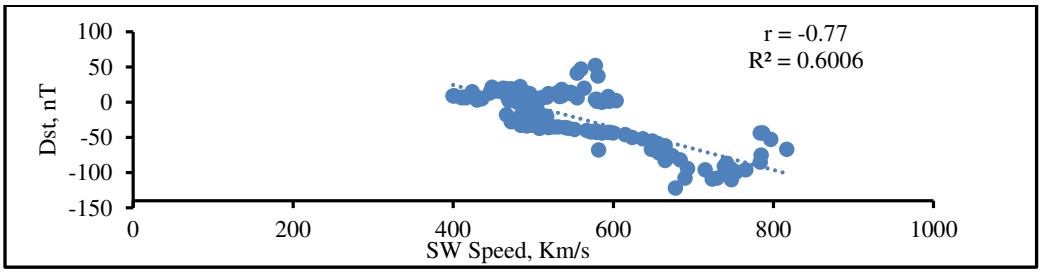

Fig.9(b)

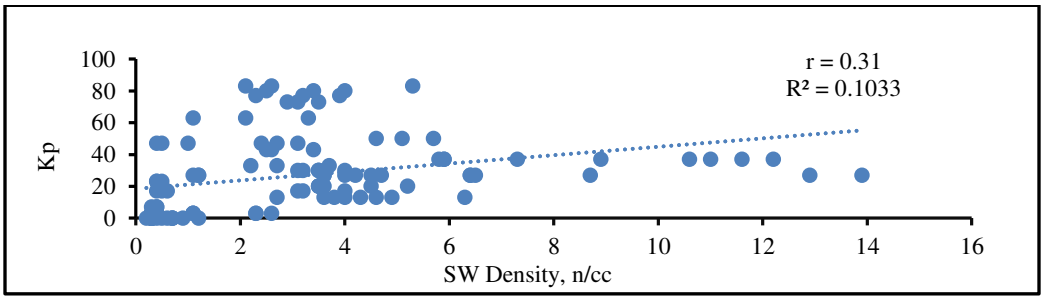

Fig.9(c)

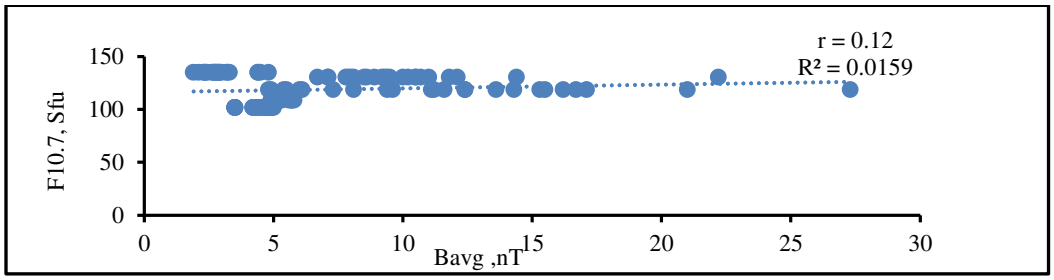

Fig.9(d)

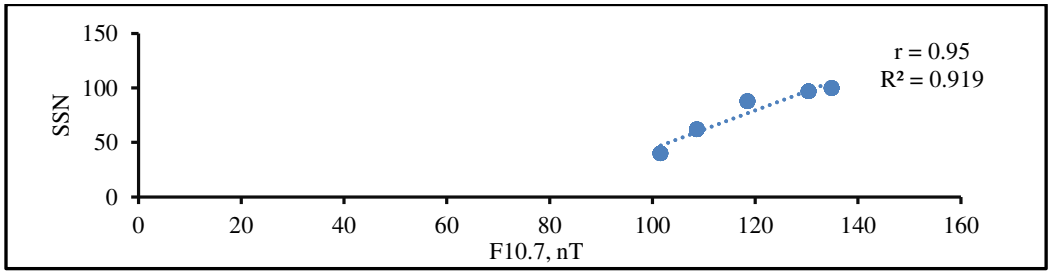

Fig.9(e)

Fig. 9. Correlation coefficient plot of daily observed values of interplanetary parameters and geomagnetic indices for (a) Bavg vs. Dst; (b) SW speed vs. Dst; (c) proton density vs. Kp; (d) Bavg vs. F10.7; (e) correlation plots of SSN vs. F10.7 during the period 05-10 Sep, 2017.

Figure 9(a) displays the inbetween the IMF Bavg and the geomagnetic storm index Dst. There is a negative correlation between these characteristics, and the value of the correlation coefficient is -0.49.Figure 9(b) displays the relationship between SW speed and the Dst index. There is a positive correlation between the two of these characteristics. These two parameters have a coefficient of correlation of 0.77. The graph displays the solar wind speed's maximum values against a negative Dst value. With a large range of velocities ranging lie between 450- 800 km/s, the scatter is greater. Peak Dst values of -124 nT for strong geomagnetic storms are better correlated with higher solar wind velocity. It has been determined that there is a positive association between solar wind speed and Dst[20].The SW proton density is shown against the planetary index Kp in Figure 9(c). There is a weak correlation between the two of these characteristics. These two parameters have a correlation value of 0.31. Therelationship between IMF Bavg and solar flare index F10.7 is depicted in Figure 9(d). There is a weak correlation between the two of these characteristics, with a value of 0.12.It has been determined that there is a positive association between sunspot number and solar flux (F10.7), and the value of the correlation is 0.95.

3.4 Solar Activity 26th August 2018

Geomagnetic storms were detected on August 26, 2018, with Dst < - 175 nT peaking at 23:00 UT. ICME also plays a major role for intense storms. A partial HALO CME with a speed of 230 km/s was seen on August 24, 2018, at 1.48 UT. The backside of the shock wave is referred to as the sheath area, which decreases the DST index and ICME values [3]. On August 24, 2018, a HALO CME linked with an B type solar flare was observed. Shock waves, strong southbound interplanetary magnetic fields, and ejecta are the primary reasons for powerful magnetic storms. On August 26, 2018, further stronger geomagnetic storms with a Dst index of -175 nT occurred. Before 6 hours of a geomagnetic storm, the average interplanetary field strength, Bavg, rapidly increases. During the storm's main phase, it fluctuates randomly for one day but returns to normal during the storm's recovery phase.

There is a strong correlation between the two of these characteristics. It is clear that higher values of solar wind density are linked to stronger geomagnetic storms. Before one day, the solar wind density increased abruptly and reached up to 17.2, while the Kp *10 index started to increase up to 73. The correlation coefficient between these indices is 0.51. Before One day, on August 25, 2018, the Bavg field increased from 5 nT to 18.1 nT, while the Kp index also rose from 7 to 73.1. During storm time, Bavg is 17.5 nT to 72.66 nT, and the solar interplanetary magnetic field increases the Kp index.

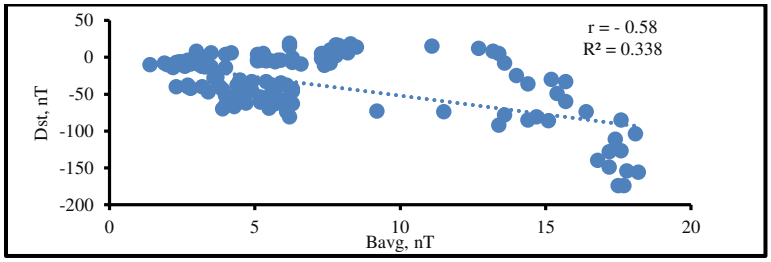

Fig.10 (a

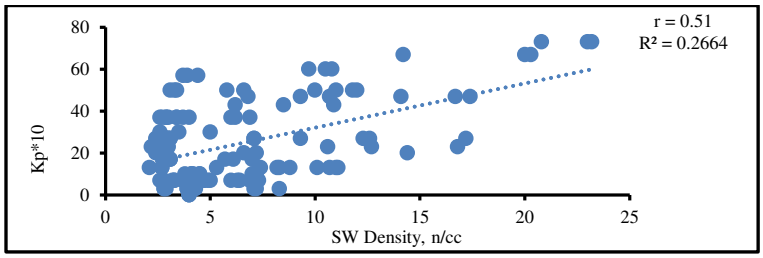

Fig.10(b)

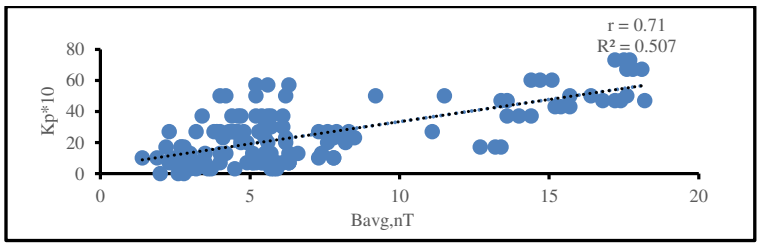

Fig.10 (c)

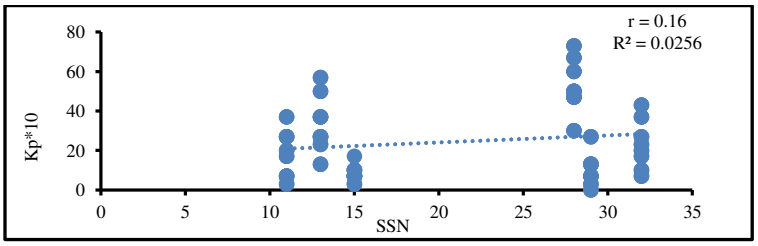

Fig.10(d)

Fig. 10 Correlation coefficient plot of daily observed values of interplanetary parameters and geomagnetic indices for (a) Bavg vs. Dst; (b) proton density vs. Kp; (c) Bavg vs. Kp; and (d) correlation plots of SSN vs. Kp during the period 23-28 August 2018.

Figure 10(a) displays the relationship between the IMF Bavg and the highest Dst (negative). There is a negative correlation(r~ -0.58) between these two characteristics. The SW proton density is shown against the planetary index Kp in Figure 10(b). There is an average correlation value 0.51 between the two of these characteristics. Figure 10(c) displays the relationship between the IMF Bavg and the Kp index. There is a strong positive correlation between the two of these characteristics. These two parameters have a correlation value of 0.71. Figure 10(d) displays the Sunspot Number (SSN) in relation to the Kp geomagnetic index have weak correlation (r~ 0.16).

Table2. represents the correlation coefficient of various interplanetary parameters observed during last phase of cycle 24

S.No	Sun Activity parameter	Major storms event time span	R^2	Correlation coefficient(r)
Storms activity March,2015				
1	Bavg & Dst	14-19 March	0.1463	-0.65
2	SW Speed & Dst		0.5231	- 0.72
3.	SW Density &Dst		0.4179	0.65
4.	SW Density &PC		0.0612	- 0.24
Storms activity December, 2015				
5.	Bavg & Dst	18-23 December	0.5256	-0.72
6.	Bavg & PC		0.5080	0.71
7.	SW Density & AE		0.3309	0.57
8.	Bavg & AE		0.3959	0.62
Storms activity September ,2017				
9.	Bavg & Dst	05-11 Sep	0.2471	-0.49
10.	SW Speed & Dst		0.6006	- 0.77
11.	SW Density & Kp		0.1033	0.31
13.	Bavg & F10.7		0.0159	0.12
14.	SSN & F10.7		0.9190	0.95

Table 3.**represents the correlation coefficient of various interplanetary parameters observed during August,2018**

Storms Activity August, 2018			R2	r
15.	Bavg & Dst	23-28 August	0.3380	-0.58
16.	SW Density & Kp		0.2664	0.51
17.	Bavg & Kp		0.5070	0.71
18.	SSN & Kp		0.0256	0.16

The above table data shows a number of solar activity characteristics and their association indices with large storm occurrences in last phase of 24 sun cycle.

In examining the large geomagnetic storms, the classification is based on the respective values of Dst< -100 nT. The correlation coefficients between SW Speed and Dst index have large values(> 0.70) show strong correlation. The Bavg and Dst variables demonstrated moderate correlation coefficients.
In the current study, we investigated how different geo indices, such as Ap, Kp, and Dst, relate to the average IMF (Bavg), solar wind proton density, and SSN. Dst value has a substantial negative correlation with Vsw, Nsw,Bz, and Bavg for all events. On the contrary, a strong positive correlation between Kp and Bavg was observed. During peak time of storms observed that the IMF (Bavg) has a substantial correlation with PC on days with great storms, as opposed to the moderate geomagnetic period.The main planetary disruption is brought onby CMEs and fast-speed solar winds, which also energise solar energetic particles and speed up ring current, aurora electrojet, and particle precipitation in the earth's atmosphere.

These quantitative data are very useful for the investigation of different models and phenomena related to space weather. The findings will provide valuable insights into the relationships between interplanetary conditions and geomagnetic storm activity, contributing to the broader understanding of space weather dynamics.

4.0 Conclusion

The study intends to examine the relationships and interplay between interplanetary factors and the frequency of severe geomagnetic storms. We examined the various activities of large geomagnetic storms having |Dst|<-100 nT for year 2015,2017 and 2018, and indescending phase of 24 cycles, using data from the Omni web-based system. The March ,2015 storm exhibited a two-step sequence, with the first minimum originating from the sheath region behind the shock and the second from the MCand Ejecta. However, it appears that the interaction of two consecutive ICMEs in space triggered these storms. Similar to this, we found that stronger geomagnetic storms happen more frequently during the sun cycle's descending phase than during its ascending phase. The study found that solar wind speed plays a significant role in causing major storm, however most storms occur at speeds between 350 - 750 km/s. Due to average solar wind speed growth, we can only estimate the advent of magnetic storms, but not their ferocity.The correlation coefficient between the solar wind speed (SW speed) and the disturbance storm time index (Dst) ranges > than 0.70show strong correlation. The interplanetary magnetic field average (Bavg) and Dst exhibit a negative correlation with an average value. There exists a positive association between proton density and AE with SW speed, whereas SSN and “F10.7” exhibit a strong positive correlation above 0.90. In this analysis, Kp is also a significant index to determinant for large geomagnetic activity. The results will offer vital insights into the connections between solar wind and disturbance features, hence enhancing the overall comprehension of space weather dynamics.

This analysis will helpful to a better analysis of the physical processes and mechanisms driving geomagnetic storm activity. The study aims to evaluate the practical implications of the findings for space weather forecasting and will explore how a better understanding of the interconnections between interplanetary parameters and geomagnetic storms can enhance the accuracy of predictions and improve mitigation strategies for safeguarding critical infrastructure, such as satellite operations, power grids, and communication networks.

Acknowledgments

The OMNI data were retrieved from the website located at http://omniweb.gsfc.nasa.gov. We truly appreciate the data support provided by various NOAA and NASA online data centres. NASA and The Catholic University of America generate and maintain the SOHO/LASCO CME catalogue at the CDAW Data Centre in collaboration with the Naval Research Laboratory.

References

1. Akasofu, S. I. (1983). Geophysical Journal International, Evolution of ideas in solar-terrestrial physics. *74*(1), 257-299. ..
2. Baker, D. N. (2000). Journal of Atmospheric and Solar-Terrestrial Physics, Effects of the Sun on the Earth's environment. *62*(17-18), 1669-1681
3. S Singh, A Pandey, K Singh and A Mishra(2012) Characteristic Features of Geomagnetic Storms Observed During Maxima of Solar Cycle 24. Int. J. Phys. Astron. 26 1103
4. Borovsky, J. E., & Shprits, Y. Y. (2017). Research in Astronomy and Astrophysics, 2015.Is the Dst index sufficient to define all geospace storms?. x*122*(11), 11-543.
5. Singh Sham, D Shrivastava and A Mishra(2012) Effect of Solar and Interplanetary Disturbances on Space-weather. Indian J. Sei. Res. 3 121
6. Singh, Sham, and A. P. Mishra(2015)"Interaction of solar plasma near-Earth with reference to geomagnetic storms during maxima of solar cycle 24. Indian Journal of Physics 89, 1227-1234
7. Burlaga, L. F., et al. (1981). Journal of Geophysical Research: Space Physics, Magnetic Loop Behind an Interplanetary Shock: Voyager, Helios, and IMP 8 Observations. 86(A8), 6673-6684.
8. SinghSham, Kalpana Singh, Ajay Vasishth, A. C. Panday, Shabir Ahmad Shabir & A. P. Mishra (2017) IJSRSET, Effect of Geomagnetic Storms and Their Association with Solar Wind Velocity during 1996-2016. 3(5), 456-460.
9. Escher, E., Gonzalez, W. D., Tsurutani, B. T., & Gonzalez, A. C. (2008). Journal of Geophysical Research: Space Physics,Interplanetary conditions cause intense geomagnetic storms (Dst≤− 100 nT) during solar cycle 23 (1996–2006). *113*(A5).
10. Singh, Sham, and A. P. Mishra(2019) "Cosmic ray intensity increases during high solar activity period for the solar cycles 22 and 23." Indian Journal of Physics 93 139-145
11. Gonzalez, W. D., Joselyn, J. A., Kamide, Y., Kroehl, H. W., Rostoker, G., Tsurutani, B. T., & Vasyliunas, V. M. (1994). Journal of Geophysical Research: Space Physics.What is a geomagnetic storm? 99(A4):5771–5792. 1991
12. Gonzalez, W. D., Tsurutani, B. T., Lepping, R. P., & Schwenn, R. (2002). . Journal of Atmospheric and Solar-Terrestrial Physics,Interplanetary phenomena associated with very intense geomagnetic storms *64*(2), 173-181.
13. Sham Singh, Ajay Vasishth, Bikramjit Singh, A. C. Panday, A. P. Mishra (2017).IJSRST, The Plasma Approximation. 3 (1), 108-117.
14. Gopalswamy, N. (2016). Geoscience Letters,History and development of coronal mass ejections as a key player in the solar terrestrial relationship. *3*(1), 1-18.
15. Gopalswamy, N., Yashiro, S., Michalek, G., Stenborg, G., Vourlidas, A., Freeland, S., & Howard, R. (2009). Earth, Moon, and Planets The soho/Lasco cme catalog. , *104*, 295-313. www.researchgate.net
16. Gosling, J. T., D. J. McComas, J. L. Phillips, S. J. Bame, J. V. Olson. in Journal of Geophysical Research: Space Physics. Geomagnetic Activity Earth Passage of Interplanetary Shock Disturbances and Solar Wind Modulation. 96(A5):7831–7839 .

17. King, J. H., & Papitashvili, N. E. (2005). Journal of Geophysical Research: Space Physics, Solar Wind Spatial Scales in and Comparisons of hourly Wind and ACE Plasma and Magnetic Field Data. 110(A2), A02209.
18. Knipp et al. 2016; Board, S. S., & National Research Council. (2009). Severe space weather events: Understanding societal and economic impacts: A workshop report. National Academies Press. ISBN:978-0-309-12769-1.
19. Mansilla, G. A. (2008). Physica Scripta, Solar wind and IMF parameters associated with geomagnetic storms with Dst<-50 nT. *78*(4), 045902.
20. Marov, M. Y. (2020). Acta AstronauticalRadiation and space flights safety: An insight., *176*, 580-590.
21. Pokharia, M., Prasad, L., Bhoj, C. et al. J Astrophys Astron, A comparative study of geomagnetic storms for solar cycles 23 and 24. **42**, 98 (2021).
22. Sham Singh, A. C. Panday, Kalpana Singh & A. P. Mishra (2017). International Journal of Pure and Applied Physics, Effect of geomagnetic storms and their association with solar wind velocity and IMF during solar cycle 23 and 24*.,* 13-1, 35-43.
23. Shreedevi, P. R., Choudhary, R. K., Thampi, S. V., Yadav, S., Pant, T. K., Yu, Y., ... & Sinha, A. K. (2020). J *Space Weather*, Geomagnetic storm-induced plasma density enhancements in the southern polar ionospheric region: A comparative study using St. Patrick's Day storms of 2013 and 2015. *18*(8), e2019SW002383.
24. Singh, A., Rao, S.S., Rathore, V.S. *et al.Space Weather*,Effect of intense solar flares on TEC variation at low-latitude station Varanasi. J Astrophys Astron**41**, 19 (2020).
25. Soraas, F., Aarsnes, K., Oksavik, K., Sandanger, M. I., Evans, D. S., & Greer, M. S. (2004). . Journal of atmospheric and solar-terrestrial physic Evidence for particle injection as the cause of Dst reduction during HILDCAA event*s*, *66*(2), 177-186.
26. Tan, B., Lin, Y., Perez, J. D., & Wang, X. Y. (2011). Journal of Geophysical Research: Space Physics, Global-scale hybrid simulation of dayside magnetic reconnection under southward IMF: Structure and evolution of reconnection. *116*(A2).
27. Tariq, S., Nawaz, H., Qayyum, F. *et al.* J Astrophys Astron , A study of the passage of high-speed solar wind streams, their plasma/field properties and space weather effects of geomagnetic disturbances. **42**, 98 (2021).
28. Temmer, M. (2021). Living Reviews in Solar Physics, Space weather: the solar perspective: An update to Schwenn (2006). *18*(1), 4.
29. Tripathi, R., & Mishra, A. P. (2010, February). Journal of Physics: Conference SeriesSolar and interplanetary disturbances responsible for geomagnetic storms. (Vol. 208, No. 1, p. 012068). IOP Publishing.
30. Varotsou, A., Friedel, R. H., Reeves, G. D., Lavraud, B., Skoug, R. M., Cayton, T. E., & Bourdarie, S. (2008). Journal of atmospheric and solar-terrestrial physics Characterization of relativistic electron flux rise times during the recovery phase of geomagnetic storms as measured by the NS41 GPS satellite. , *70*(14), 1745-1759.